Journal of Medicinal Chemistry

Article

Docking Studies and Ligand Recognition in Folylpolyglutamate Synthetase

Xiao-Jian Tan, and Heather A. Carlson

J. Med. Chem., **2005**, 48 (24), 7764-7772• DOI: 10.1021/jm0507734 • Publication Date (Web): 01 November 2005

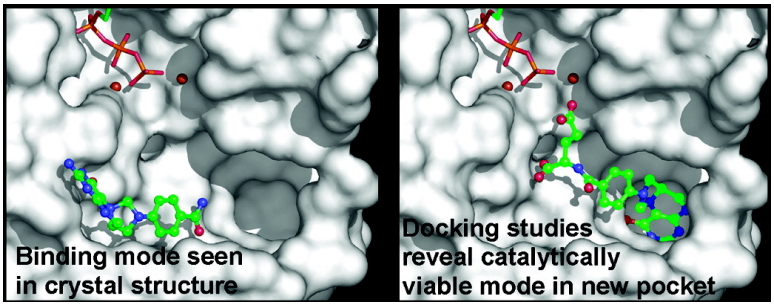

More About This Article

Additional resources and features associated with this article are available within the HTML version:

- Supporting Information
- Links to the 2 articles that cite this article, as of the time of this article download
- Access to high resolution figures
- Links to articles and content related to this article
- Copyright permission to reproduce figures and/or text from this article

View the Full Text HTML

Journal of Medicinal Chemistry is published by the American Chemical Society. 1155 Sixteenth Street N.W., Washington, DC 20036

Docking Studies and Ligand Recognition in Folylpolyglutamate Synthetase

Xiao-Jian Tan and Heather A. Carlson*

Department of Medicinal Chemistry, College of Pharmacy, University of Michigan, 428 Church St., Ann Arbor, Michigan 48109-1065

Received August 5, 2005

Folylpolyglutamate synthetase (FPGS) catalyzes the sequential addition of several glutamates to folate, forming γ-linked polyglutamate folates of varying lengths. To understand how this protein is capable of accommodating ligands of different length and net charge, we have performed docking studies for folate substrates and glutamate based on the ternary crystal structure of *Lactobacillus casei* FPGS. Our results suggest two locations for folate binding, the one seen in the crystal structure and another distinct cavity. According to our model and experimental data, it is highly probable that folate can bind in both sites, and we suggest that the new pocket is especially important for the initial addition of the first glutamate residue. Docking longer substrates, di- and triglutamylated folates, showed how these molecules bind in the same sites. The longer folates also adopted transition-state-like conformations that may help us to understand the ligation reaction in FPGS and influence the design of mechanism-based inhibitors for anticancer or antimicrobial therapy.

Introduction

Folate cofactors play an essential role in a number of metabolic processes, where they serve as carriers of one-carbon units in the biosynthesis of purines, thymidylate, glycine, and methionine.[1] After folates are absorbed into the cell, they are rapidly metabolized to folylpoly-γ-glutamates. Folylpoly-γ-glutamates are poorly accepted by the membrane carriers responsible for efflux, so polyglutamated folates accumulate and maintain the cellular folate pool.[2] Furthermore, polyglutamate folates are preferred substrates for many folate-dependent enzymes. Both in bacteria and eukaryotes, folylpoly-glutamate synthetase (FPGS) catalyzes the addition of the glutamates to folate. Due to its importance in folate metabolism, FPGS has become a target for cancer chemotherapy.[3,4]

The FPGS reaction mechanism (Figure 1) involves the activation of folate's terminal γ-carboxylate group by ATP, forming an acyl phosphate intermediate.[5,6] The intermediate undergoes a nucleophilic attack by the amine of glutamate to form a peptide bond. In the case of *Lactobacillus casei* FPGS, up to 11 glutamate residues can be subsequently added.[7,8] The fact that the protein is capable of recognizing folate derivatives of various lengths and net charges is particularly interesting. Three crystal structures of *L. casei* FPGS have been reported.[9,10] One contains its preferred substrate 5,10-methylenetetrahydrofolate (mTHF) and an adenosine-5′-[β,γ-methylene]-tetraphosphate (ACP_4), which was formed by phosphorylation of the cofactor mimic adenosine-5′-[β,γ-methylene]-triphosphate.[10] Crystal structures, CD spectra, and EPR studies have shown that binding mTHF and ATP results in a conformational change of the protein.[10,11] Our studies have focused on this reactive conformation seen in the ternary crystal structure (FPGS·mTHF·ACP_4).

The protein is capable of recognizing folate derivatives of various lengths and net charges, but the binding modes of polyglutamate folates are unknown. In the complex structure, only part of the mTHF molecule was resolved, but it appears that its γ-carboxylate group would be too far from the catalytic center to participate in the reaction. Also, the binding site of the incoming L-glutamate has not been determined in structural studies (NMR or crystallography). In this study, we have used docking calculations to probe the modes of binding for folate, polyglutamylated folates, and the attacking glutamate.

Results

Detailed summaries of the docking results are provided in the Supporting Information. Tables provide docking scores and list all residues within 3 Å of the most favorable docked poses. Coordinates are also given.

Docking to the FPGS·ACP_4 Model. In the ternary crystal structure, the cofactor mimic ACP_4 was bound. Our main goal for studies using the FPGS·ACP_4 model was to reproduce the position for folate seen in the crystal structure and verify our methodology. mTHF and the pteroyl moiety (the resolved portion of mTHF seen in the crystal structure with FPGS·ACP_4) were docked to the model and successfully reproduced the binding conformation seen in the crystal structure of the complex. Therefore, our protocol should be appropriate for the other docking simulations of the FPGS system.

For the pteroyl moiety, the largest cluster was in good agreement with the position in the crystal structure. For mTHF, its pterin rings formed hydrogen bonds with the backbone of F75 and the side chain of R82 and S417, as seen in the crystal structure. It also participated in nonpolar interactions with residues F75, F121, and Y414. The cluster contained poses with many different orientations of the glutamate tail of mTHF, indicating its flexibility, as is consistent with the unresolved

* To whom correspondence should be addressed. Tel: (734) 615-6841. Fax: (734) 763-2022. E-mail: carlsonh@umich.edu.

10.1021/jm0507734 CCC: $30.25
Published on Web 11/01/2005

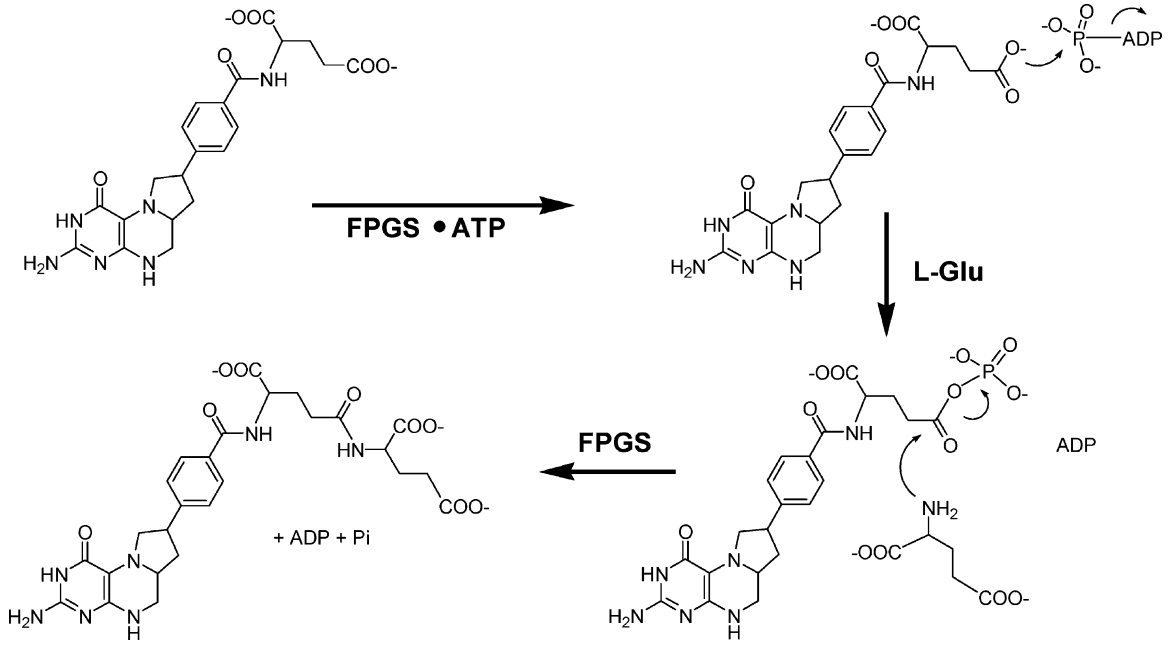

Figure 1. The mechanism of the ligation reaction catalyzed by FPGS.

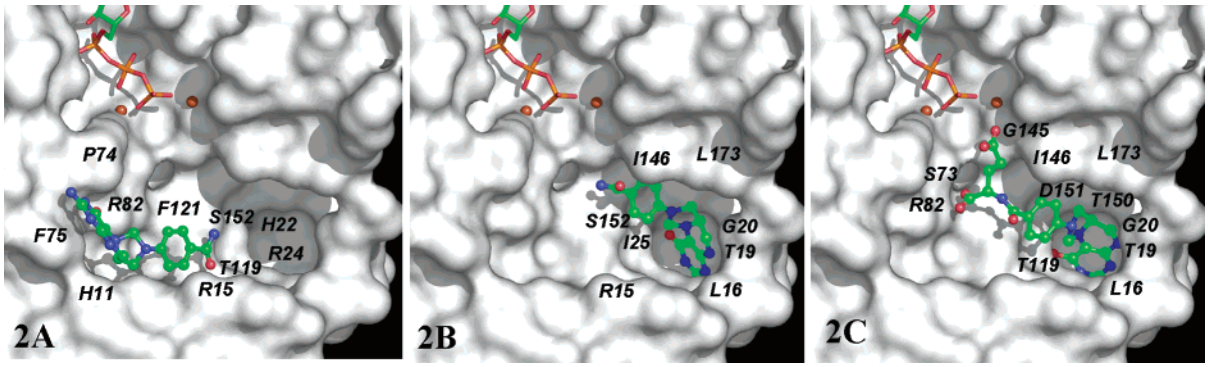

Figure 2. Binding modes of the pteroyl moiety and mTHF within the FPGS·ATP model. (A) The pteroyl moiety bound in the binding site seen in the crystal structure. (B) The pteroyl moiety bound in the new pocket. (C) The reactive binding mode of mTHF in the new pocket with the γ-carboxylate near ATP. The folate substrates are shown in ball-and-stick, ATP in stick, and Mg^{2+} shown by two brown spheres. For clarity, all hydrogen atoms are hidden, and only the surface of the N-terminal domain is shown. The protein surface is the same in all figures and labeled with N-terminal FPGS residues. It was not possible to clearly label all key residues in all figures.

glutamate tail in the crystal structure. Even in the most favorable poses, the γ-carboxylate group of mTHF was still quite far from the reaction center, suggesting a nonproductive binding mode. Unexpectedly, we observed quite a few poses of mTHF and the pteroyl moiety distributed in another distinct binding site (described in more detail in the docking studies based on FPGS·ATP). While bound in this new pocket, the glutamate tail of mTHF still could not approach the vicinity of the ACP_4 and Mg^{2+}. It appeared that the δ-phosphate of ACP_4 was blocking the appropriate position for the folate tail, preventing the γ-carboxylate of mTHF from occupying that position during the docking calculations. Our calculations suggest that the Coulombic repulsion of the additional, fourth phosphate on ACP_4 may be the reason that the crystal structure did not yield a "reactive" conformation of mTHF.

Docking the Pteroyl Moiety and mTHF to FPGS·ATP. The proper cofactor for FPGS is ATP, and the FPGS·ATP model was used to gain insight into the catalytically active system. Docking the pteroyl moiety and mTHF to the FPGS·ATP model identified poses in both the crystallographic position and the new pocket. The two binding modes seen for the pteroyl moiety and mTHF are shown in Figure 2. The docking energies indicated that the poses in the new pocket were slightly more favorable than the crystal poses (ΔE_{dock} of 2.7 kcal/mol for the pteroyl moiety and 0.9 kcal/mol for mTHF).

In docking the pteroyl moiety, the protein−ligand interactions of the crystal pose were similar to those of the FPGS·ACP_4 model (Figure 2A). In the new binding pocket (Figure 2B), the pteroyl moiety formed hydrogen bonds with T19, G20, and S152. The ligand also appeared to have general hydrophobic interactions with side chains and backbones of residues 18−25 that make up a large portion of the new pocket. Several clusters of binding conformations were observed for the pteroyl moiety in the new pocket. Over the conformations, reorientation of the pterin rings and twisting of the benzymidal ring resulted in positions for the terminal amide functionality that swept out a wide arc, ranging 6−12 Å away from the terminal phosphate of ATP. The different orientations of the pteroyl moiety in these

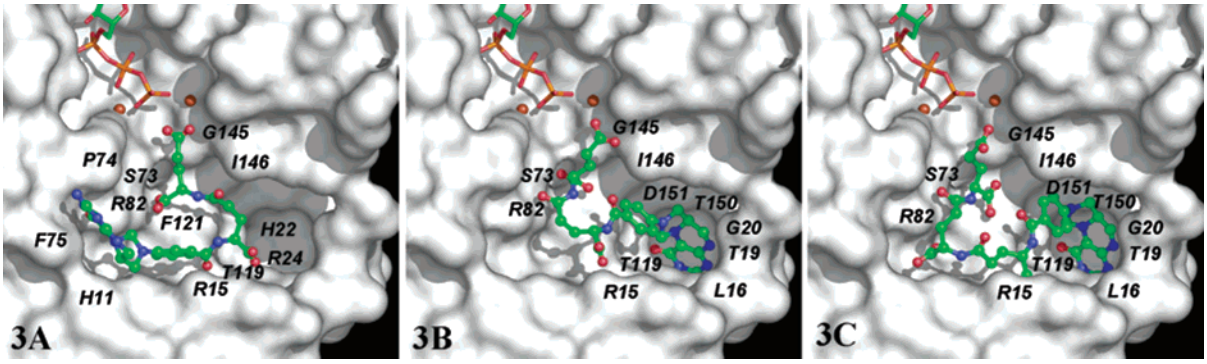

Figure 3. Catalytically productive binding modes of diglutamate and triglutamate substrates where the γ-carboxylate is near ATP. (A) Diglutamate substrate bound in the crystal position. (B) Diglutamate substrate bound in the new pocket. (C) Triglutamate substrate bound in the new pocket.

clusters may be suitable for accommodating different lengths of glutamate chains.

For mTHF bound in the new pocket (Figure 2C), the pteroyl moiety still associated with residues 18−25 and had additional hydrogen bonds with T150, D151, and S152. The α-carboxylate group of the glutamate tail formed hydrogen bonds with residues R82 and S73, and the γ-carboxylate group interacted with the catalytic Mg^{2+} close to the ATP and the hydroxyl of Y414 (C-terminal residues are not shown in Figure 2). This is an appropriate position to allow the initial phosphorylation of the γ-carboxylate. However, all calculated conformations of mTHF in the crystal position were unable to place the glutamate tail close enough to the ATP and Mg^{2+} ions for catalysis.

Docking Polyglutamate Folates to FPGS·ATP. Dockings of diglutamate (5,10-CH_2−H_4PteGlu$_2$) and triglutamate (5,10-CH_2−H_4PteGlu$_3$) substrates were only conducted with the FPGS·ATP model. In docking the diglutamate substrate, both crystal and new-pocket poses were examined. Again, the new-pocket poses were estimated to be slightly more favorable than those in the crystal poses. However, the results of docking the diglutamate substrate indicated that both pockets were capable of binding the longer folate in a reactive mode, placing the γ-carboxylate close to the ATP (Figure 3A,B). When docked to the position from the crystal structure (Figure 3A), the pteroyl moiety remained at the same location, associated with P74, F75, and S417 (S417 is a C-terminal residue not shown in Figure 3). The second α-carboxylate of the diglutamate tail was hydrogen bound to R82 while the terminal γ-carboxylate bound to the catalytic Mg^{2+}. For the new-pocket poses, the interactions seen for the pteroyl group of mTHF were reproduced with the longer folates. The first α-carboxylate of the diglutamate tail was hydrogen bonded to R15; the second α-carboxylate formed hydrogen bonds with R82 and S73. The terminal γ-carboxylate bound to Mg^{2+}. Consistent with the spread of poses found for the pteroyl moiety in the new pocket, we found that the pteroyl group of the longer folates twisted slightly to provide enough space for the additional glutamate chain.

Due to the high flexibility of the triglutamate substrate, more variation in the docked poses was obtained. The second-ranked cluster had a very favorable docking score (−21.6 kcal/mol) and bound in a reactive mode with the pteroyl moiety in the new pocket and the γ-carboxylate associated with the catalytic magnesium ion. As shown in Figure 3C, the pteroyl group twisted even further within the pocket, resulting in an orientation more suitable for accommodating the longer glutamate chain. The protein−ligand interactions for the poses in the new pocket included the common pattern for the pteroyl group interacting with residues 18−25 and 150−152. The first α-carboxylate hydrogen bonded with the backbone of residues 119−122 and the side chain of R15. The second and third α-carboxylates formed hydrogen bonds with R82 and S73. The terminal γ-carboxylate associated with the hydroxyl of Y414 and the catalytic Mg^{2+} is appropriate for catalyzing the ligation reaction.

Conversely, glutamate tails were randomly orientated for the crystal poses. It was not clear whether it was due to insufficient sampling or because the position seen in the crystal structure was a poor binding site for the triglutamate substrate. It was very difficult to find a reactive conformer, but a single pose in the 139th cluster appeared to be an appropriate conformation for catalysis with the γ-carboxylate located near the catalytic magnesium ion. However, the score for this conformer was 7.6 kcal/mol poorer than the reactive, new-pocket pose.

Docking L-Glutamate to FPGS·ATP. Given the catalytic mechanism,[6] one could expect to find at least two major binding sites for glutamate, one for the folate tail and one for the attacking glutamate. Several binding modes were observed from docking glutamate. The first ranked cluster contained the largest number of poses and represented the folate-tail position. Glutamate in this cluster formed hydrogen bonds with R82, S73, and Y414 and a salt bridge with the catalytic Mg^{2+}. The positions of the two carboxylate groups were roughly the same as those of the mTHF pose in the new pocket, but it was the α-carboxylate instead of the γ-carboxylate group approaching ATP and Mg^{2+}. Several catalytically feasible, tail-like poses (where the γ-carboxylate approached the ATP, as shown in Figure 4A) were found in the seventh-ranked cluster (containing 11 poses). The misorientation seen for the first cluster, where the α-carboxylate approached ATP rather than the γ-carboxylate, may possibly be caused by the presence of an ammonium group in L-glutamate. As part of the folate tail, the nitrogen is part of an amide and neutral. Also, the presence of the pteroyl rings may bias the orientation and make it more favorable to orient the γ-car-

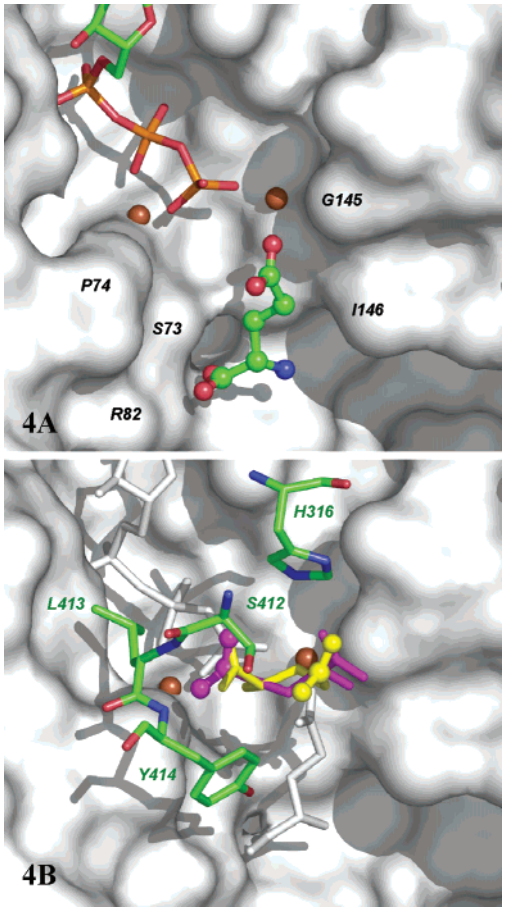

Figure 4. Glutamate binding modes. (A) Folate-tail pose; residues in the N-terminus that provide the surface contacts are labeled in black. (B) Two possible orientations for the attacking glutamate (the γ-carboxylates are shown in ball-and-stick); the pose in yellow is more favorable than the one in magenta. Four key residues from the C-terminus are shown in stick models and labeled in green text. ATP and the tail glutamate are colored in white to help the reader focus on more relevant features.

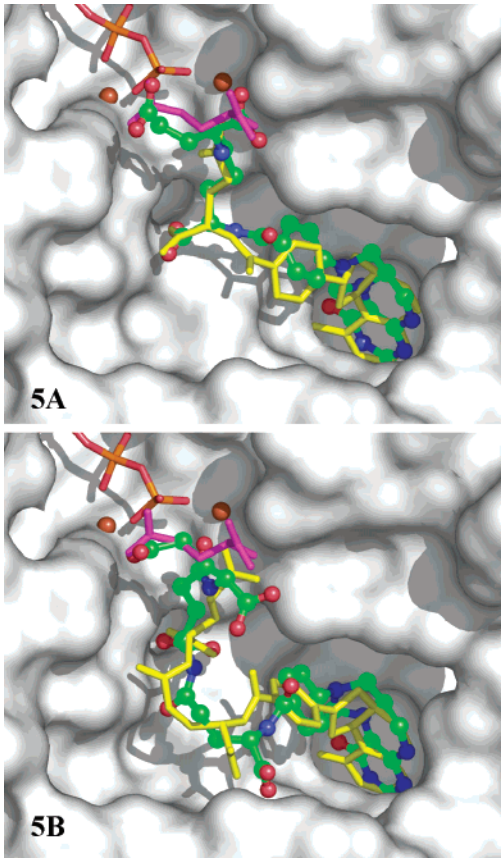

Figure 5. Poses resembling binding modes for transition states or products. The protein surface is not labeled with residues, but the orientation is the same as Figures 2−4, and the contacts are the same. (A) Diglutamate substrate TS-like pose (ball-and-stick model) superimposed onto mTHF in its reactive binding mode (stick model, in yellow) and the attacking glutamate (stick model, in magenta). (B) Triglutamate substrate in a TS-like pose superimposed onto the diglutamate substrate in its reactive binding mode and the attacking glutamate (using similar stick models).

boxylate toward the ATP. Only one binding pose in a very low-ranked cluster resembled the attacking glutamate.

During the reaction, both the glutamate tail and the attacking glutamate must be present at the same time. The folate binds before the glutamate,[6,11] and its presence may bias the location of the attacking glutamate. To verify this view and find the real attacking-glutamate binding mode, we performed another docking calculation in the presence of a "tail glutamate" (a FPGS·ATP·Glu model like Figure 4A). A single "tail glutamate"—with the γ-carboxylate oriented toward the ATP·Mg^{2+} center—was chosen over a full folate molecule so that the position identified for the attacking glutamate was independent of any choice between the two folate binding sites. In the presence of a tail, the second-ranked and largest cluster of docked glutamates was appropriate for an attacking conformation. In this binding mode (yellow model in Figure 4B), the ammonium of glutamate is hydrogen bonded to the γ-carboxylate of the tail and the γ-phosphate of ATP. The γ-carboxylate of the attacking glutamate associated with H316 and S412; the α-carboxylate formed hydrogen bonds with the backbone of L413 and the backbone and side chain of Y414. The 19th-ranked cluster was similar to the most favorable poses, except that the glutamate was flipped and the two carboxylate groups were interchanged (magenta model in Figure 4B). This pose was also bound between residues H316, S412, L413, and Y414. The flip in its orientation still placed the attacking nitrogen against the γ-carboxylate of the tail, but on the face opposite of the ATP. This second binding mode could be recognized as an alternative attacking-glutamate conformation.

Poses That Resemble Transition States or Products. In both diglutamate and triglutamate substrate dockings, poses that resembled transition states (TS) or products were observed. These conformations had terminal glutamates bound in the location of the "attacking L-Glu" described above. Most TS-like poses were found in the new binding pocket. For the diglutamate substrate, the TS-like poses were actually the top-ranked, largest cluster (the reactive pose in the new pocket was ranked second and the crystal pose was ranked 10th). The pteroyl rings and the first glutamate moiety of 5,10-CH_2−H_4PteGlu_2 adopted a binding mode similar to mTHF in the new pocket, and the last glutamate in the tail occupied roughly the same position as we determined for the attacking glutamate (Figure 5A). A similar result was also found for the triglutamate substrate, where the last glutamate occupied the at-

tacking-glutamate position (Figure 5B). In Figure 5, the most favorable docked conformers placed the γ-carboxylate toward ATP (like the magenta model in Figure 4B). However, it was noted that in the collection of TS-like poses, the terminal glutamate could adopt orientations where either its γ-carboxylate or α-carboxylate was oriented toward ATP.

The triglutamate substrate was also capable of adopting a TS-like pose while the pteroyl group occupied the position seen in the crystal structure (a TS-like, crystal pose). However, this was a single conformer in the 96th-ranked cluster. The docking score for the TS-like pose in the new pocket was 5.6 kcal/mol more favorable than the TS-like, crystal pose.

Discussion

Which Binding Site Is Correct? Our docking studies revealed two distinct binding sites for folate substrates. One is observed in the crystal structure, but the other is in a new pocket that was never previously reported to be involved in catalysis or substrate recognition.

As noted by the crystallographers,[10] the resolved pteroyl rings of mTHF are too far away from the catalytic center to allow for its initial turnover. The benzamidyl group is >10 Å away from the catalytic site in the crystal structure, which could accommodate a diglutamate substrate for catalysis but not a monoglutamate folate.[10] Our mTHF docking results showed that the γ-glutamate could not approach the reaction center when the pteroyl moiety occupied the location seen in the crystal structure. Naturally, the question becomes, how does FPGS fulfill the first and subsequent turnovers? It was suggested in the crystallographic study[10] that the initial glutamylation of mTHF might require an additional conformational change, possibly involving the Ω-loop. Our new binding site suggests another possibility.

Other experimental data suggests the possibility of two folate binding sites. Fluorinated methotrexate inhibitors synthesized by Coward and co-workers undergo one glutamylation, but inhibit further ligation reactions.[12] If the specificity of the initial ligation is different than subsequent turnovers, this could indicate a different binding site. Preliminary data produced by Bognar and co-workers for other inhibitors of FPGS indicate noncompetitive inhibition,[13] implying that a second binding site may exist. Furthermore, the *met-6* mutation of FPGS from *Neurospora crassa* will catalyze the first turnover, but not additional ligations.[14]

After our calculations were completed, crystal structures of *Escherichia coli* FolC were published.[15] *E. coli* FolC is a bifunctional enzyme that creates dihydrofolate through the amide ligation of glutamate and dihydropteroate. It also adds additional glutamates to the dihydrofolate product, forming folylpolyglutamates. It has only one ATP binding site, and the same catalytic center promotes the same chemistry (both reactions involve the nucleophilic attack of a glutamate amine onto a phosphorylated carboxylate intermediate[6]). It was proposed that the dual activity may come from different binding modes for different ligands. The dihydropteroyl-phosphate in the crystal structure of *E. coli* FolC occupies a new pocket that is very similar to our own. Dihydropteroyl-phosphate is the phosphorylated intermediate for the first turnover, which creates dihydrofolate in FolC.[6] Its position and orientation are very similar to those of mTHF bound in our new pocket. Structural superposition of *E. coli* FolC and *L. casei* FPGS (Figure 6) revealed that the pocket in FolC is smaller, but they share several conserved residues. T119, F121, E122, G145, and D151 in *L. casei* FPGS are equivalent to T122, F124, E125, G148, and D154 in *E. coli* FolC. Those residues are proximal to the catalytic center and help accommodate the glutamate tail region of mTHF. The nonconserved residues in the deeper part of the new pocket interact with the pteroyl portion of mTHF and dihydropteroate. These residues may be responsible for the different shapes of the binding sites and the differing substrate specificity. The larger pocket in *L. casei* FPGS is appropriate for accommodating its longer substrates.

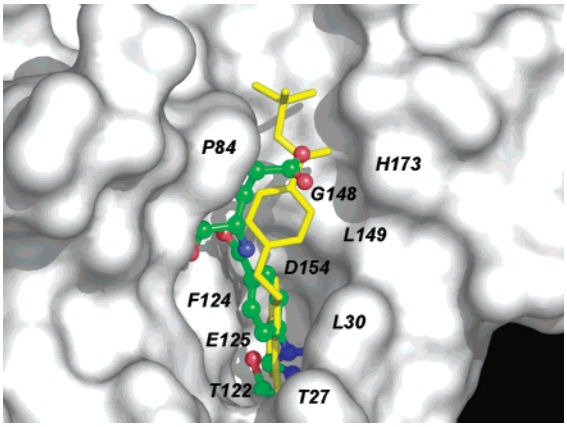

Figure 6. Crystal structure of *E. coli* FolC with ADP and dihydropteroyl-phosphate (pdb code 1W78)[15] superimposed upon our model of *L. casei* FPGS·ATP with mTHF in the new pocket. Only the pteroyl ligands and the surface of the N-terminal domain of *E. coli* FolC are shown. The protein surface is labeled with key residues in *E. coli* FolC. Our model (mTHF) is shown in ball-and-stick and colored by element; the dihydropteroyl-phosphate in FolC is shown as yellow sticks.

Further support of the new pocket is the observation of TS-like poses. Both diglutamate and triglutamate substrates are capable of adopting poses resembling a TS or postligation product. These poses imply that a reactive conformation of substrates is possible when folate or monoglutamylated folate binds in the new pocket. A TS-like pose was seen when the pteroyl rings occupied a crystal pose, but only the longer triglutamate ligand was able to take that confirmation. Again, this supports the hypothesis that the crystal pose does not allow the initial turnover. The TS-like poses identified in this study may aid the understanding of the ligation reaction, especially the initial turnover of mTHF. They may also help in the design of mechanistic-based inhibitors.

It should be emphasized that the binding site of mTHF seen in the crystal structure cannot be completely ruled out. Data on the aforementioned inhibitors may imply that a second site is important in the inhibition of FPGS.[12,13] Also, the crystal poses located with the di- and triglutamate substrates show that the position can accommodate folates. Though the crystal poses are ranked lower in this study of the shorter folates, they could be more important for longer folylpoly-

glutamates with 5−10 γ-glutamates. The binding site in the crystal structure is much more solvent-exposed. This would allow for greater variation of ligand size and less desolvation penalty for the large number of charges found in the longer tails. It may explain how *L. casei* FPGS can add up to 11 glutamates to the folate, accommodating ligands of greatly varying length and net charge.

The Position of the Attacking L-Glutamate. Two binding sites were found for L-glutamate, one appropriate for the folate tail and the other for the attacking glutamate. The "tail-glutamate" position was supported by docking full folates. The TS-like poses of the di- and triglutamate substrates provided some support for the "attacking-glutamate" position. Mutagenesis studies indicated the importance of H316, S412, and Y414 in binding the attacking glutamate. The S412A mutant of *L. casei* FPGS increased the K_M for L-glutamate by ~60-fold.[16] Mutant H338A of human FPGS (equivalent to His316 in *L. casei* FPGS) led to a 600-fold increases of the K_M for L-glutamate.[17] The Y414A mutant of *L. casei* FPGS raised the K_M value for L-glutamate by 60-fold.[13] The attacking-glutamate poses found in our docking study clearly revealed association of glutamate between these three residues.

Experiments have shown that glutamate is unable to bind the free enzyme and does not cause any conformational changes, but binding folate (and ATP) results in protein domain movement.[11] This conformational change brings residues H316, S412, and Y414 closer to the active site, forming the binding site of glutamate. We found that, even with the proper protein conformation, it was still difficult to obtain the attacking-glutamate binding mode. Only in the presence of the glutamate tail (folate) was the attacking mode preferred. Hence in this view, folate binding to FPGS not only plays a role in protein conformational change, but also induces glutamate binding.

We should note that our model of ATP and the glutamate tail is an obvious simplification. Folates are the appropriate substrate, and it is always possible that the attacking glutamate binds after phosphorylation of the glutamate tail. But even with our simplified model, the position appears to agree well with mutagenesis data.

Processing Several Turnovers in the New Binding Site. Figure 7 presents docked poses from this study that demonstrate how the first two turnovers may be processed by FPGS (and how the first three substrates can be bound in an active conformation in the new pocket). An interesting feature is the interaction of α-carboxylates with R82/S73 and R15. For the first turnover, the α-carboxylate closest to the pterin interacts with R82/S73. After the attacking glutamate is added, it becomes the terminal glutamate and must be located between the catalytic magnesium and R82/S73 to be in a reactive orientation. This means that the first α-carboxylate (noted as α_1 in Figure 7) must move away from R82/S73. It appears that R15 is essential to complementing the α-carboxylates closest to the pterin as the chain lengthens.

Conclusion

Our docking studies of *L. casei* FPGS indicate that there are two possible sites for binding folate substrates. One has been observed in the crystal structure of the FPGS·ACP_4·mTHF complex, and the other is a newly identified cavity. The di- and triglutamate substrates can be accommodated in both sites in a way appropriate for the ligation reaction, but only the new pocket appears to bind mTHF and allow the initial ligation reaction. We suggest that the new pocket plays an essential role in the first turnover to create folylpolyglutamates. Our studies show that the new pocket can also allow subsequent turnovers and that R15 (and R82/S73) are important in complementing the growing glutamate chain. However, we are unable to determine how very long folates are bound to FPGS. It may be possible to gain insight into the binding of longer substrates in future studies that incorporate protein flexibility and domain motion.

The experimental evidence, especially a recent crystal structure of *E. coli* FolC,[15] confirms the importance of our new pocket. FolC is a bifunctional enzyme that catalyzes the formation of dihydrofolate and then adds several additional glutamates to create folylpolyglutamate products. The first turnover for FolC is the production of dihydrofolate, and the new pocket is implicated in the first turnover (in keeping with our hypothesis that the new pocket is important in the first turnover of *L. casei* FPGS). However, the authors of the FolC structural study note that humans and *L. casei* do not synthesize folates and the production of dihydrofolate is unique to certain bacteria. Since the new site is used for dihydrofolate production in FolC, it was hypothesize that the new pocket may be a specific target for antimicrobial therapies. Our study shows that the new site may also be used for FPGS activity. The new site may still be very important for specific inhibitors for antimicrobial vs anticancer therapies, because our docking studies and the FolC structure show that it is the site of recognition of the pteroyl moiety. The enzymes from different species bind different folates preferentially. The new binding site has many nonconserved residues that might be responsible for the altered specificity, making the new site a rich landscape for structure-based designs that target bacterial vs human enzymes.

We have also proposed a position for the attacking glutamate, based on docking glutamate, the diglutamate substrate, and the triglutamate substrate. The interactions between the protein and the attacking glutamate are consistent with experimental studies. The attacking glutamate has not been observed in structural studies, so these calculations provide new insights into the mechanism. Furthermore, TS-like poses for the di- and triglutamate ligands may be useful in the design of mechanism-based inhibitors.

We are working with our collaborators to design experiments to probe the hypotheses presented from these docking studies.

Computational Methods

Model Preparation. The computational models of FPGS were based on the ternary crystal structure of FPGS, ACP_4, and the resolved pteroyl moiety of mTHF (PDB code 1JBW).[10] Small unresolved regions in 1JBW were built on the basis of the binary complex of FPGS with the cofactor ATP (PDB code 1JBV).[10] However, there was a larger unresolved loop in both FPGS structures—G378-G385—which had to be modeled on

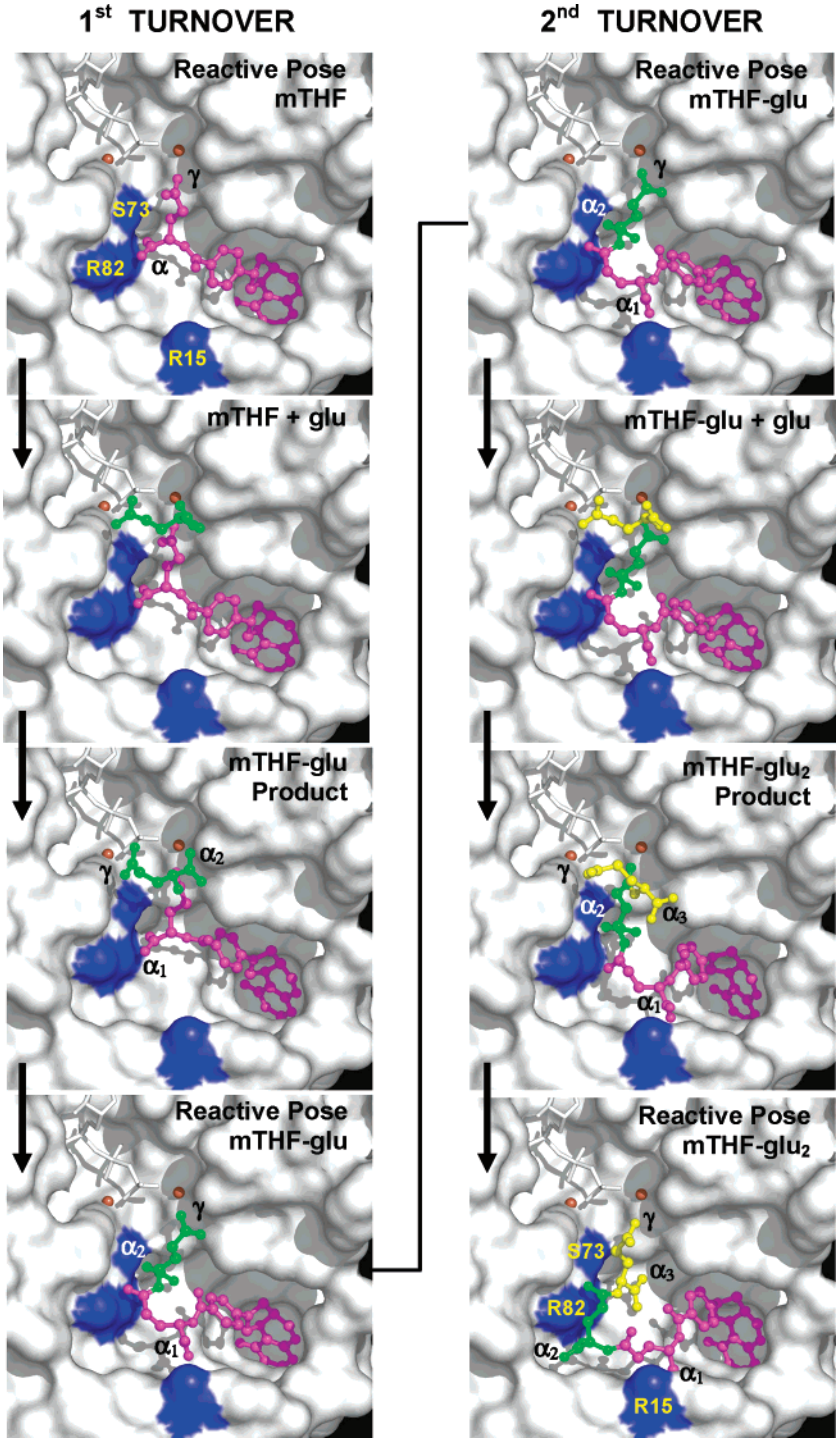

Figure 7. Proposed first and second turnover in the new pocket. The key side chains of R15, S73, and R82 are colored in blue. The initial mTHF is in magenta; the first attacking L-Glu is in green, and second attacking L-Glu is in yellow. The terminal γ-carboxylate and α-carboxylates are labeled to help the reader follow the reorganization of the growing folate product.

the basis of the homologous protein MurE (PDB code 1E8C).[18] This region is far from the active site. The most notable issue in building the missing loop based on MurE's backbone was the fact that the side chain of R386 in the FPGS structure was in excellent agreement with the backbone of MurE. It appeared that the density of neighboring backbone atoms in the FPGS structure was misassigned as the R386 side chain. Therefore, we reoriented the R386 side chain as was appropriate for the MurE structure. During the buildup of missing regions, structures were aligned with an emphasis on matching adjacent secondary structures in the local area.

MOE[19] was used for structural alignments, adding hydrogens, building unresolved residues, and performing energy minimizations. The AMBER94 force field[20] was used with our own parameters for polyphosphates for ATP.[21] FPGS contains a modified residue, a carbamylated K185 (a KCX residue). PEOE charges[22] were used for K185 and ACP_4. HIS protonation states were carefully determined by checking the surrounding electrostatic potentials. A 10-Å cutoff was used for van der Waals and electrostatic interactions; a distance-dependent dielectric was used. In general, the backbone was not minimized, except in the regions where the 1JBV and 1E8C structures were used to fill in the unresolved regions in the 1JBW structure. Added side chains were also subjected to short energy minimizations. The short minimizations consisted of 200 steps of steepest descent.

Two models were created: one containing ACP_4, like the crystal structure, and one containing ATP, the proper cofactor.

To create a model of FPGS with ATP bound, ACP_4 was modified and one of the two Mg^{2+} (Mg2) was moved to the position seen in 1JBV and homologous enzymes. In both structures, all hydrogens were minimized. Side chains and backbones of all residues within 6 Å of ACP_4/ATP and the two Mg^{2+} ions were minimized. (The cofactor and the magnesium ions were allowed to move during the minimization.) The minimization used 200 steps of steepest descent, followed by conjugate gradient until the rms gradient became less than 0.01 kcal/mol.

Docking Studies. For each protein model, ATP (or ACP_4) and two magnesium ions were included in the structure. Autodock 3.05[23] was used in the docking studies. Autodock requires the user to assign united-atom charges. Only polar hydrogen atoms were kept with AMBER united-atom charges[24] assigned by MOE.[19] For ligands, cofactors (ATP and ACP_4), and the modified K185, charges of carbons were altered to include their nonpolar hydrogens as appropriate for a united-atom representation. Our ligands included the pteroyl moiety, mTHF, the diglutamate substrate, the triglutamate substrate, and L-glutamate. United-atom representations were used, and PEOE charges were assigned by MOE. Charges for the ligands and cofactors are given in the Supporting Information.

The same docking box (same size and grid center) was used for both models, and grid spacing was 0.3 Å. Docking experiments were performed using the Lamarckian genetic algorithm (LGA) with flexible ligands and rigid proteins. We modified the default docking parameters as follows: maximal mutation of 1 Å in translation and 5° in rotation and orientation. Simulations were carried out with a population size of 100 and a maximum of 5 million energy evaluations (for the triglutamate substrates docking, a maximum of 10 million energy evaluations was employed because of the large number of rotatable bonds). Final docked conformations were clustered using a tolerance of 1.5 Å rmsd. Each docking was performed at least 100 times, yielding 100 or more docked conformations.

For the FPGS·ACP_4 model, our main goal was to reproduce the conformation in the crystal structure and show that our parameters and chosen protocol were appropriate. Therefore, only the pteroyl moiety and mTHF were considered in the docking study with FPGS·ACP_4. Since ATP is the true cofactor, our docking studies of folates and glutamate focused on the FPGS·ATP model. Docking the pteroyl moiety and mTHF from random starting positions revealed two dominating binding sites. For longer folates, the large number of rotatable bonds required that we do more focused sampling to reach convergence. The longer folates were initially placed in the two positions identified with the pteroyl moiety and mTHF, and then we initiated conformational sampling with LGA. The docking results were then combined for ranking and clustering.

Figures 2−7 were made using Pymol.[25]

Acknowledgment. The authors would like to thank Prof. James K. Coward (University of Michigan, Ann Arbor) and Prof. Andrew L. Bognar (University of Toronto) for helpful discussions and sharing their data prior to publication. We would also like to thank Dr. Mavinahalli N. Jagadeesh for his initial work on this project. We are grateful to Prof. Arthur J. Olson (Scripps Research Institute, La Jolla) for providing us with the Autodock program. This work has been supported by the National Institutes of Health (GM 65372) and the Beckman Young Investigator Program.

Appendix

Abbreviations. FPGS, folylpolyglutamate synthetase; pteroyl moiety, 5,10-methylenetetrahydropteroylamide; mTHF, 5,10-methylenetetrahydrofolate or 5,10-CH_2−H_4PteGlu; ACP_4, adenosine-5′-[β,γ-methylene]-tetraphosphate; diglutamate substrate, 5,10-CH_2−H_4PteGlu$_2$; triglutamate substrate, 5,10-CH_2−H_4PteGlu$_3$; MurE, UDP-*N*-acetylmuramyl tripeptide synthetase; TS, transition state.

Supporting Information Available: Detailed docking information of selected binding modes for each substrate, united-atom charges for unusual molecules, and coordinates of the best poses. This material is available free of charge via the Internet at http://pubs.acs.org.

References

(1) Cossins, E. A. The fascinating world of folate and one-carbon metabolism. *Can. J. Bot.* **2000**, *78*, 691−708.
(2) Shane, B. Folylpolyglutamate synthesis and role in the regulation of one-carbon metabolism. *Vit. Horm.* **1989**, *45*, 263−335.
(3) McGuire, J. J.; Coward, J. K. Folylpolyglutamate synthetase as a target for therapeutic intervention. *Drugs Future* **2003**, *28*, 967−974.
(4) Gangjee, A.; Dubash, N. P.; Zeng, Y.; McGuire, J. J. Recent advances in the chemistry and biology of folypoly-γ-glutamate synthetase substrates and inhibitors. *Curr. Med. Chem.* **2002**, *2*, 331−355.
(5) Shane, B. Pteroylpoly(γ-glutamate) synthesis by *Corynebacterium* species. Studies on the mechanism of folypoly(γ-glutamate) synthetase. *J. Biol. Chem.* **1980**, *255*, 5663−5667.
(6) Banerjee, R. V.; Shane, B.; McGuire, J. J.; Coward, J. K. Dihydrofolate synthetase and folylpolyglutamate synthetase: Direct evidence for intervention of acyl phosphate intermediates. *Biochemistry* **1988**, *27*, 9062−9070.
(7) Shane, B.; Bognar, A. L.; Goldfarb, R. D.; Lebowitz, J. H. Regulation of folypoly-γ-glutamate synthesis in bacteria: In vivo and in vitro synthesis of pteroylpoly-γ-glutamates by *Lactobacillus casei* and *Streptococcus faecalis*. *J. Bacteriol.* **1983**, *153*, 316−325.
(8) Toy, J.; Bognar, A. L. Mutagenesis of the *Lactobacillus casei* folylpolyglutamate synthetase gene at essential residues resembling and ATP binding site. *Arch. Biochem. Biophys.* **1994**, *314*, 344−350.
(9) Sun, X.; Bognar, A. L.; Baker, E. N.; Smith, C. A. Structural homologies with ATP- and folate-binding enzymes in the crystal structure of folylpolyglutamate synthetase. *Proc. Natl. Acad. Sci. U.S.A.* **1998**, *95*, 6647−6652.
(10) Sun, X.; Cross, J. A.; Bognar, A. L.; Baker, E. N.; Smith, C. A. Folate-binding triggers the activation of folylpolyglutamate synthetase. *J. Mol. Biol.* **2001**, *310*, 1067−1078.
(11) Sheng, Y.; Ip, H.; Liu, J.; Davidson, A.; Bognar, A. L. Binding of ATP as well as tetrahydrofolate induces conformational changes in *Lactobacillus casei* folylpolyglutamate synthetase in solution. *Biochemistry* **2003**, *42*, 1537−1543.
(12) McGuire, J. J.; Hart, B. P.; Haile, W. H.; Rhee, M. S.; Galivan, J.; Coward, J. K. DL-β,β-Difluoroglutamic acid mediates position-dependent enhancement or termination of pteroylpoly(γ-glutamate) synthesis catalyzed by folylpolyglutamate synthetase. *Arch. Biochem. Biophys.* **1995**, *321*, 319−328.
(13) Bognar, A. L. University of Toronto, unpublished results.
(14) Atkinson, I. J.; Nargang, F. E.; Cossins, E. A. Folylpolyglutamate synthesis in *Neurospora crassa*: Primary structure of the folylpolyglutamate synthetase gene and elucidation of the *met-6* mutation. *Phytochemistry* **1998**, *49*, 2221−2232.
(15) Mathieu, M.; Debousker, G.; Vincent, S.; Viviani, F.; Bamas-Jacques, N.; Mikol, V. *Escherichia coli* FolC structure reveals an unexpected dihydrofolate binding site providing an attractive target for antimicrobial therapy. *J. Biol. Chem.* **2005**, *280*, 18916−18922.
(16) Sheng, Y.; Sun, X.; Shen, Y.; Bognar, A. L.; Baker, E. N.; Smith, C. A. Structural and functional similarities in the ADP-forming amide bond ligase superfamily: Implications for a substrate-induced conformational change in folylpolyglutamate synthetase. *J. Mol. Biol.* **2000**, *302*, 427−440.
(17) Sanghani, S. P.; Sanghani, P. C.; Moran, R. G. Identification of three key active site residues in the C-terminal domain of human recombinant folylpoly-γ-glutamate synthetase by site-directed mutagenesis. *J. Biol. Chem.* **1999**, *274*, 27018−27027.
(18) Gordon, E. J.; Flouret, B.; Chantalat, L.; van Heijenoort, J.; Mengin-Lecreulx, D.; Dideberg, O. Crystal structure of UDP-*N*-acetylmuramoyl-L-alanyl-D-glutamate: *meso*-Diaminopimelate ligase from *Escherichia coli*. *J. Biol. Chem.* **2001**, *276*, 10999−11006.
(19) *Molecular Operating Environment (MOE),* Version 2003.02; Chemical Computing Group Inc.: Montreal, Quebec, Canada, 2003.
(20) Cornell, W. D.; Cieplak, P.; Bayly, C. I.; Gould, I. R.; Merz, K. M.; Ferguson, D. M.; Spellmeyer, D. C.; Fox, T.; Caldwell, J. W.; Kollman, P. A. A second generation force field for the simulation of proteins, nucleic acids, and organic molecules. *J. Am. Chem. Soc.* **1995**, *117*, 5179−5197.

(21) Meagher, K. L.; Redman, L. T.; Carlson, H. A. Development of polyphosphate parameters for use with the AMBER force field. *J. Comput. Chem.* **2003**, *24*, 1016−1025.
(22) Gasteiger, J.; Marsili, M. Iterative partial equalization of orbital electronegativity—A rapid access to atomic charges. *Tetrahedron* **1980**, *36*, 3219−3228.
(23) Morris, G. M.; Goodsell, D. S.; Halliday, R. S.; Huey, R.; Hart, W. E.; Belew, R. K.; Olson, A. J. Automated docking using a Lamarckian genetic algorithm and an empirical binding free energy function. *J. Comput. Chem.* **1998**, *19*, 1639−1662.
(24) Weiner, S. J.; Kollman, P. A.; Case, D. A.; Singh, U. C.; Ghio, C.; Alagona, G.; Profeta, S.; Weiner, P. A new force-field for molecular mechanical simulation of nucleic-acids and proteins. *J. Am. Chem. Soc.* **1984**, *106*, 765−784.
(25) DeLano, W. L. *PyMOL molecular graphics system*; DeLano Scientific: San Carlos, CA, 2002.

JM0507734